Applied Biochemistry and Biotechnology (2023) 195:2786–2802
https://doi.org/10.1007/s12010-022-04249-0

ORIGINAL ARTICLE

Human Papillomavirus E1 Protein Regulates Gene Expression in Cells Involved in Immune Response

Zifeng Wang[1] · Shimin Guan[1] · Baoguo Cai[1] · Shaofeng Rong[1] · Qianqian Li[1]

Accepted: 8 November 2022 / Published online: 23 November 2022
© The Author(s), under exclusive licence to Springer Science+Business Media, LLC, part of Springer Nature 2022

Abstract

Human papillomavirus belongs to papovaviridae family papillomavirus A, a spherical deoxyribonucleic acid (DNA) virus, which can cause the proliferation of squamous epithelial cells of human skin or mucous membranes. With the rapid increase in the incidence of condyloma acuminatum among STDs and the increase in diseases caused by HPV infection, HPV infection has seriously endangered human health. In this paper, the in vitro detection of HPV E1 protein was realized using AgNCs-dsDNA. And through the test of this detection method, we calculated that the detection limit of this method is 0.886 nM. Compared with other methods for detecting E1 protein in vitro, this method has high sensitivity and simple operation. In addition, the detection method also has good anti-interference and selectivity, and can realize the detection of E1 in serum samples. The transfection efficiency of BLV-miR-B4-3p mimics at different time points was determined by quantitative real-time PCR (qPCR); the transcriptome sequencing of lymphocytes transfected with different concentrations of BLV-miR-B4-3p mimics was performed, and differential gene clustering was performed on the sequencing results. And the BLV-miR-B4-3p target gene prediction and transcriptome analysis results were verified by qPCR. The effects of BLV-miR-B4-3p on the transcriptional levels of immune-related cytokines in human lymphocytes were analyzed. Transcriptome sequencing analysis showed that after BLV-miR-B4-3p entered lymphocytes, a total of 556 differentially expressed genes were obtained. GO enrichment and KEGG analysis results showed that BLV-miR-B4-3p could independently activate influenza. The signaling pathway ultimately affects the body's immune system process, stress response, defense response, immune response, and other biological processes. After BLV-miR-B4-3p enters lymphocytes, it will lead to abnormal lymphocyte immune function, including the mRNA expression of TNF-α in Th1 cytokines which was significantly increased ($P<0.05$), and the expression of IL-10 in Th2 cytokines was significantly increased ($P<0.05$). The mRNA expression was significantly decreased ($P<0.05$), and the mRNA expression of IL-27 was significantly increased ($P<0.001$), which did not affect the mRNA expression of lymphocyte proliferation and activation-related regulators. The tumor suppressor breast cancer 1 (BRCA1) and antimicrobial peptide CAMP were significantly increased, and decreased ($P<0.001$), and the expression of pro-apoptotic factor Caspase9 showed a significant downward trend ($P<0.05$).

Extended author information available on the last page of the article

Keywords Immune response · Cellular gene expression · Human papillomavirus · E1 protein

Introduction

Papillomavirus is an epitheliophilic virus that is widely distributed in humans and animals with a high degree of specificity [1]. Human papillomavirus belongs to the genus papillomavirus A of the family Papillomaviridae. It is composed of closed double-stranded circular deoxyribonucleic acid (DNA) and can cause the proliferation of squamous epithelium of human skin and mucous membranes [2]. Because the host of the virus is human, it is called human papillomavirus. Human papillomavirus can cause tumors and warts in humans, such as human warts vulgaris, condyloma acuminatum, and papillomas that grow on the mucous membranes that grow on the skin near the reproductive organs [3]. Human papillomavirus is a general term for a class of viruses, and the morphology of viruses within the family is extremely similar. However, studies have shown that different types of human papillomaviruses have different DNA restriction endonuclease maps and different antigenicity of their nucleocapsid proteins. At present, there are about 80 HPV types with complete genome sequences, of which about 20 have been confirmed to infect the female reproductive tract and lead to tumorigenesis [4].

In recent years, high-risk HPV genotyping technology has become quite mature, and cervical cancer screening and prevention work has been actively promoted [5]. The incidence will be largely reduced. Analysis of high-risk HPV infection rates and HPV dominant types in women in different regions has positive clinical significance in reducing the incidence of cervical cancer, and can also provide data support for cervical cancer screening programs and preventive HPV vaccination of high-risk groups. Thus, the socioeconomic burden caused by cervical cancer can be reduced [6]. Therefore, studying the distribution of high-risk HPV infection rates and predominant types in women in different regions can provide theoretical data support for women's preventive HPV vaccination programs in different regions. High-risk HPV E1 and E7 are closely related to tumorigenesis by inducing genomic instability and promoting abnormal cell proliferation [7]. Mutations in the E1 and E7 genes result in amino acid variations that can alter virus pathogenicity, affect host immune responses, and vaccine therapeutic efficacy. Due to the gradual improvement of sequencing technology, there have been many studies on HPV gene sequences at home and abroad, which makes the data in the HPV gene database huge and can be used to infer the phylogenetic characteristics of HPV mutation sequences in the region. The construction of phylogenetic trees by comparing homologous DNA sequences is one of the main tasks of phylogenetic analysis. Studying the single nucleotide mutation sites of HPV E1 and E7 genes, analyzing the mutation characteristics of HPV gene sequences in different regions, and the pedigree distribution of variant strains are the basis for timely discovery of HPV epidemic strains in various regions and vaccine development and other HPV prevention and control measures [8].

The expression and purification of human papillomavirus HPV 16 E1 were carried out with reference to the literature method, including transformation, small test tube culture colony, high-dose culture colony, bacterial collection, protein purification, and other steps, are the same as the literature method. The summary is as follows: In order to improve the monodispersity of the E1 protein, the wild-type E1 sequence was mutated, and the recombinant HPV16 E1 4C/4S was expressed in *E. coli*. In this paper, after further TEM

characterization, the phenomenon of fluorescence enhancement and blue shift was attributed to AgNCs-electrostatic interaction between dsDNA and HPV E1 protein and the interaction between AgNCs-dsDNA and cysteine in HPV E1 protein, and the interaction between AgNCs-dsDNA and cysteine in HPV E1 protein predominates. This provides a new method for the detection of HPV E1 protein in vitro. The mature sequences of BLV-miRNAs were obtained from the mirbase website, and the miRanDa software was used to predict, analyze, and verify the target gene functions of BLV miRNAs. BLV-miR-B4-3p, which has the risk of regulating human diseases (leukemia, breast cancer), was selected as the research object, and BLV-miR-B4-3p with different transfection doses was analyzed and verified by transcriptomic methods on the gene expression of human lymphocytes. The effects of different transfected amounts of BLV-miR-B4-3p on the expression of Th1 type, Th2 type, and lymphocyte proliferation and activation-related cytokines in human lymphocytes were detected and analyzed by quantitative real-time PCR (qPCR). Through experiments, we have proved that the detection method has good sensitivity, good selectivity, and anti-interference, and can also be detected in serum samples. Through the research in this chapter, we have enriched the biological applications of AgNCs-dsDNA. When BLV-miR-B4-3p is taken up by lymphocytes, it will reduce the expression of antibacterial and antiviral-related genes in lymphocytes, resulting in abnormal transcription of inflammatory factors in lymphocytes in a concentration-dependent manner.

Materials and Methods

Preparation of AgNCs-dsDNA

DNA-protected silver nanoclusters (AgNCs-dsDNA) usually consist of less than 20 silver atoms and have the advantages of ultra-small size, low toxicity, and good biocompatibility. Therefore, AgNCs-dsDNA has received extensive attention in the fields of photochemistry, bioimaging, biodetection, and biosensing.

The preparation of AgNCs-dsDNA mainly refers to the previous reports of our group. The process can be summarized as follows: two pieces of single-stranded DNA are mixed in a 1:1 molar ratio, heated in an oil bath at 92 °C for 6 min, and then quenched to allow the single-stranded DNA to hybridize into double-stranded DNA. After that, the sample tube containing the double-stranded DNA was cooled at room temperature for 1 h, and sodium borohydride and phosphate-buffered solution were added to it; after mixing it evenly, it was allowed to stand at room temperature for 25 min; then an equal amount of nitric acid was added. Silver was vortexed for 2 min. After overnight at room temperature, it was stored in the refrigerator at 3 °C, and protected from light. The main instruments are shown in Table 1.

Expression and Purification of Human Papillomavirus HPV 16 E1

There are several amino acid residue gaps between the beginning and the end of the sequence, there are high variation sites in the sequence, and the intratype consistency of genotype 2a is the highest; the sequence is heavily glycosylated, and there are multiple glycosylation sites; the sequence is distributed with relatives. In the aqueous region, genotype 1b has a high score; most subtypes of genotypes 1b, 6a, 3b, and 3a have one transmembrane region, and most subtypes of genotype 2a have two transmembrane regions. There

Table 1 Main instruments

Equipment name	Instrument model	Manufacturer
CO2 incubator	MCO-20AIC	Sanyo Corporation
Haier Medical Refrigerator	HYC-310S	Qingdao Haier Biomedical Co., Ltd
Protein purification system	AKTA	Pure GE
Cell Program Cooling Box	EC06	Easyinno
Protein electrophoresis system	PAC300	Bio-rad
Cell disruptor	VCX750	SONICS
Cryogenic high-speed centrifuge	5810R	Eppendorf
Ultra low temperature refrigerator	UFV700	Binder
Incubator shaker	ZHWY-221C	Shanghai Zhicheng Instrument Co., Ltd
Inverted phase contrast microscope	TS100	Nikon
Clean bench	SW-CJ-2F	AIR TECH
Automatic cell counter	Countess II	Life technologies

are no signal peptides in genotypes 3b and 3a, and there are signal peptides in genotype 2a; there are many different modification sites and B cell antigens on the protein sequence, and there are obvious gaps between each genotype and subtype, and there is great heterogeneity. This study provides a certain scientific basis for revealing the virus infection mechanism and developing regional vaccines.

Cells were cultured at 20 °C until OD600 reached 0.8, after which target protein expression was induced by the addition of IPTG. Cells were then centrifuged and sonicated to obtain GST-E1. The GST-E1 protein fusion in the supernatant was then purified using a GST column, and the column was washed with 20 column volumes of buffer B (50 mM Tris–HCl, pH 6.8, 0.2 M NaCl, 2 mM DTT) to remove impurities. Enzyme-prescprotease (PPase, Health Guard Inc.) was then added to the column and digested at 4 °C to remove the GST tag and yield the E1 protein. The phylogenetic tree of HPV16 E1-E7 genes is shown in Fig. 1.

Identification of Proteins by Sodium Dodecyl Sulfate Polyacrylamide Gel Electrophoresis and Western Blotting

The target protein E1 was identified using Coomassie brilliant blue negative-stained sodium dodecyl sulfate polyacrylamide gel electrophoresis (SDS-PAGE) and western blotting (Western-blot). Take a 1.5-mL centrifuge tube and place it on the centrifuge tube rack, add 20 μL of the sample to be identified, and then add 5 μL of chromogenic solution; mix the two well, and then boil the sample at 95 °C for 10 min. After denaturation, the sample was centrifuged for 1 min, 10 μL of the supernatant was added to a 12% polyacrylamide gel, the gel was placed in a buffer solution, and a certain voltage was applied to make the protein band of the sample in the gel separated in. After electrophoresis, take out the separating gel on the protein gel plate, put it in a staining solution containing Coomassie brilliant blue for 20 min, and then put the separating gel in a decolorizing solution such as acetic acid to decolorize. The approximate molecular weight of the protein can be preliminarily determined by comparing the bands of the target protein with the Protein Maker.

In order to further explain that the obtained protein is the target protein, it needs to be verified by Western-blot: according to the steps of SDS-PAGE, the gel with the target

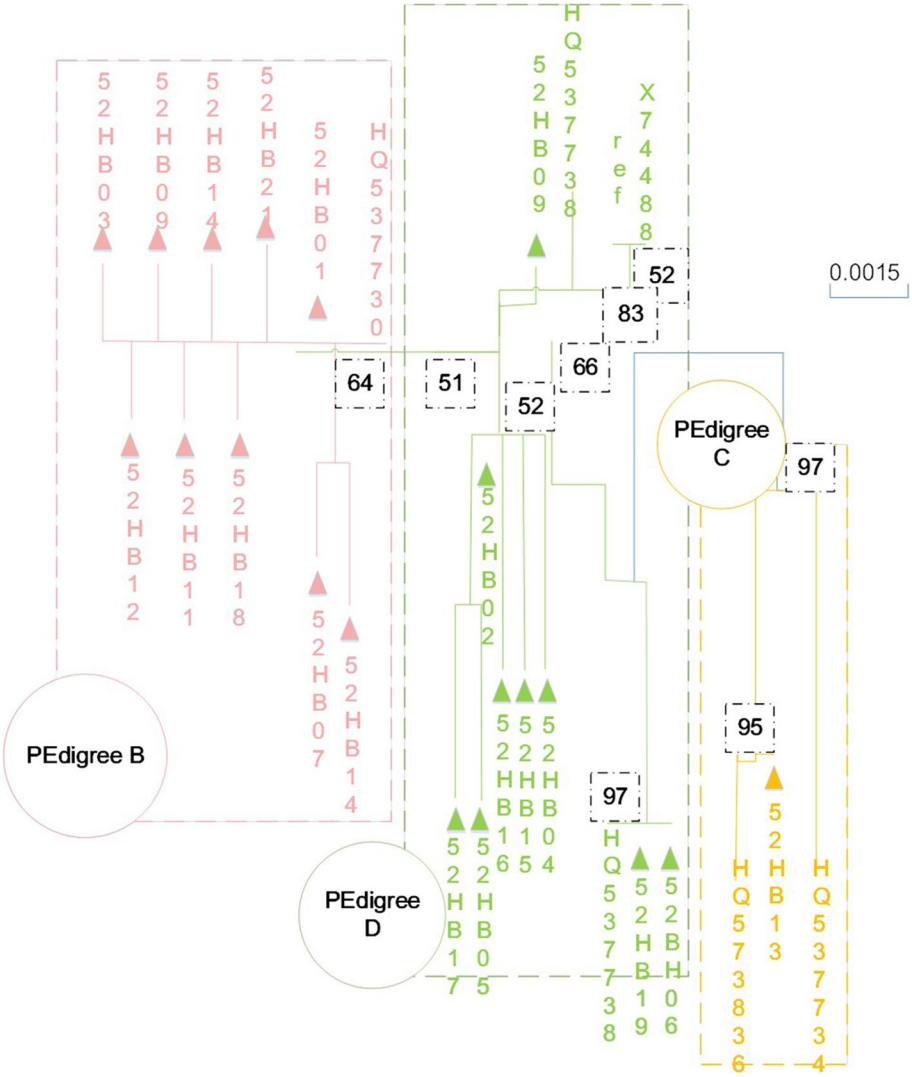

Fig. 1 Phylogenetic tree of HPV16 E1-E7 genes

protein is obtained. If there is a target protein band on the cellulose membrane, it proves that the protein is expressed successfully.

Cell Total RNA Extraction

The human lymphocytes transfected with BLV-miR-B4-3p mimics were taken out from the cell culture incubator, and the cells in the 6-well plate were blown evenly with a pipette; the culture medium containing cells was extracted and transferred to a 1.5-mL centrifuge tube. Centrifuge at 1000 rpm/min for 4 min, the cell culture medium can be added to centrifuge tubes for several times and centrifuge the cells, discard the supernatant, resuspend

the cells in 1 mL of sterile PBS, and centrifuge at 1000 rpm/min for 4 min; discard the supernatant, add 1 mL of TRIzol, pipette repeatedly for 3–5 min, and let stand for 5 min at room temperature; add 200 μL of chloroform, shake vigorously, and let stand for 2–3 min; centrifuge at 12,000 rpm/min at 4 °C 15 min; the samples after centrifugation were divided into three layers. The first layer is a colorless water-like layer, the second layer is a white intermediate layer, and the third layer is a pink organic layer. Carefully extract the upper aqueous phase and put it into a new 1.5-mL centrifuge tube; add 500 μL of isopropanol to the aqueous layer, invert and mix slowly, and let stand at room temperature for 10 min; centrifuge at 12,000 rpm/min at 4 °C for 10 min. Discard the supernatant, add 1 mL of 75% ethanol (pre-cooled) prepared with DEPC, shake evenly, and wash the pellet thoroughly. Centrifuge at 7500 rpm/min at 4 °C for 5 min; discard the supernatant; after the transient, carefully aspirate the residual supernatant. Put it upside down on the filter paper on the ultra-clean bench, turn on the ventilation, and let it dry naturally for 10–15 min. Add an appropriate amount (20–40 μL) of DEPC water to dilute the RNA and store at − 80 °C.

Transcriptomic Analysis of the Effect of BLV-miR-B4-3p on Human Lymphocytes

Blood was collected from 6 healthy volunteers in the laboratory. There was no history of alcohol consumption within 24 h and no history of drug use within 7 days before blood collection. Fifty milliliters of fresh blood was collected by professionals and stored in sterile blood collection tubes containing EDTA anticoagulant.

Take a 15-mL centrifuge tube and add 4 mL of human peripheral blood lymphocyte separation solution first. Carefully draw 4 mL of blood sample with an electric pipette, add it to the liquid surface of the separation solution, 1000 g, and centrifuge it horizontally for 40 min. After centrifugation, the liquid in the centrifuge tube is divided into four layers from top to bottom; the first layer is the plasma layer, the second layer is the annular lymphocyte layer, the third layer is the transparent separation liquid layer, and the fourth layer is the red blood cell layer.

Carefully drop the incubated mixture into the corresponding wells of the 6-well plate for lymphocyte culture, shake well, and put it back into the cell incubator for culture. After the lymphocytes were cultured in the incubator for 24 h, the 6-well cell culture plate was taken out, and the cells were collected by centrifugation in a 1.5-mL centrifuge tube, and 1 mL of TRIzol was added to lyse the cells, and stored at − 80 °C until transcriptome sequencing.

Total RNA from qualified samples was extracted as material for library preparation. First, the polyA tailed mRNA was enriched by Oligo (dT) magnetic beads, and the RNA was purified by binding buffer and washing buffer; fragmentation buffer was used to randomly break the mRNA into short RNA fragments. The fragment is reverse transcribed into a single-strand cDNA as a template; dUTP is used to replace dTTP in dNTPs, then the cDNA end is repaired, A tail is added, and the UMI tag and sequencing adapter are connected to synthesize the second-strand cDNA. The second-strand cDNA was degraded, the cDNA was amplified by PCR, and the PCR product was purified by DNA Clean Beads; finally, the PCR product was recovered by nuclease-free water.

After downloading the reference genome and genome model annotation files from the genome website, use the software Hisat2 v2.0.4 to construct the index file of the reference genome and compare it with the clean reads. We then used UMI-tools v1.0.0 to remove duplicates in the gene coordinates mapped to the reference genome and UMI reads. The process of the test statistics of the effect of BLV-miR-B4-3p on human lymphocytes is shown in Fig. 2.

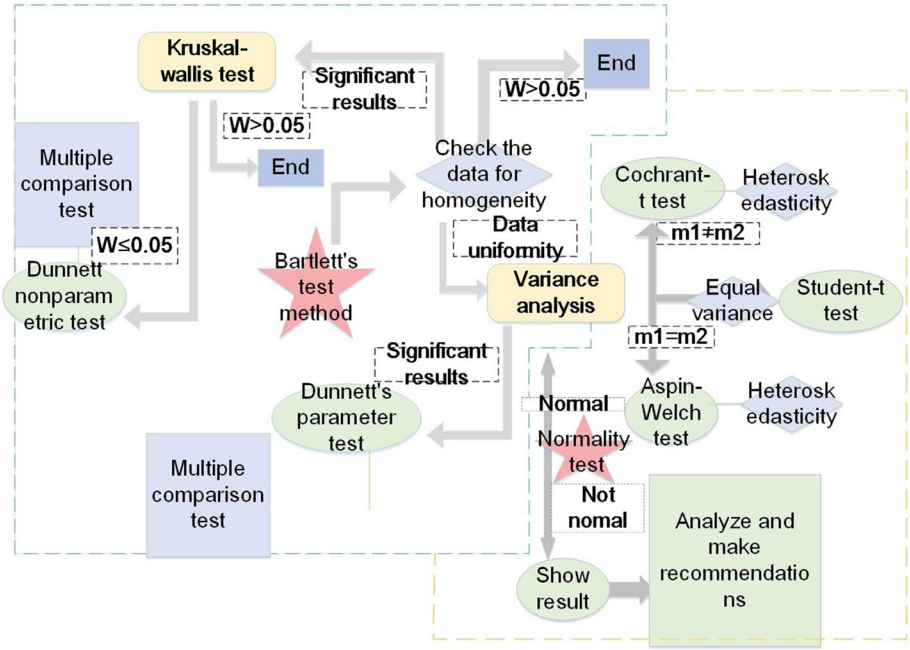

Fig. 2 The process of testing statistics for the effect of BLV-miR-B4-3p on human lymphocytes

Differential Gene Expression Analysis

DESeq is a negative binomial distribution-based model that provides statistical routines for determining differential expression of digital gene expression data. We use the DESeq package of the R package (1.18.0) software to analyze the differentially expressed genes between groups. In order to ensure that the error rate will not affect the analysis results, we use the Benjamini and Hochberg methods to proofread the *P* values of the analysis results. The number of reads of each sequencing library was adjusted by scale normalization through the edgeR package, and finally we defined $P < 0.05$ and log2 (fold change) of 1 as the threshold for significant differential expression of genes.

The GO enrichment analysis of differentially expressed genes was performed by the GOseq package, and the gene length bias was corrected. When $P < 0.05$, the corresponding GO item was finally confirmed as a significantly enriched cluster of differentially expressed genes. KEGG is a database containing advanced functions and uses of signaling pathways. We used KOBAS software to perform statistics on differentially enriched KEGG pathways.

Among the three groups of differential genes (T10 vs NC, T100 vs NC, T200 vs NC) that appeared after the comparison, we randomly selected three upregulated and downregulated genes, designed primers, and verified the mRNA expression of the differential genes by qPCR. qPCR primers were designed and synthesized online by Sangon Bioengineering (Shanghai) Co., Ltd.

Results and Analysis

Detection of HPV E1 Protein in Serum

To verify the utility of this assay in clinical diagnosis, we further used AgNCs-dsDNA to detect E1 protein in human serum. AgNCs-dsDNA (final concentration of 1.2 μM) was added to 1% serum (diluted with PB buffer, pH = 7.3), and E1 protein was gradually added dropwise to the system to test the fluorescence response of AgNCs-dsDNA and E1 protein. In 1% serum, E1 protein responded well to AgNCs-dsDNA at low concentrations (1.0–15 nM). The fluorescence response of AgNCs-dsDNA is shown in Fig. 3.

Result of AgNCs-dsDNA Detection of HPV E1 Protein

In order to further study the essential mechanism of AgNCs-dsDNA detection of E1 protein, we dismembered E1 into multiple small peptides according to its secondary structure characteristics. Then, according to the isoelectric point (PI) value of the small peptide and the secondary structure characteristics, 4 small peptides were selected and synthesized (the small peptides were designed based on the wild-type E1 protein sequence).

We added the QR small peptides to buffers containing AgNCs-dsDNA at final concentrations of 1.0 and 2.0 μM, respectively. The fluorescence spectra were tested after 20-min incubation at room temperature. Compared with AgNCs-dsDNA alone (1.0 μM), the fluorescence of the mixed solution was greatly enhanced (approximately sixfold). In order to exclude the interference of the self-luminescence of small peptides, we also tested the control sample-QR small peptide solution in parallel. It was found that the QR peptide did not fluoresce by itself in the buffer without AgNCs-dsDNA, which fully demonstrated that the fluorescence enhancement of AgNCs-dsDNA caused by the mixing of the two was due to the strong interaction between them.

We optimized the response time (Fig. 4) and mixing concentration ratio (Fig. 5) for both identifications, respectively. The time-dependent effect of fluorescence spectra showed that the fluorescence of AgNCs-dsDNA at 555 nm was rapidly enhanced and red-shifted after the two were mixed, and the change trend reached a stable steady state at about 5 min.

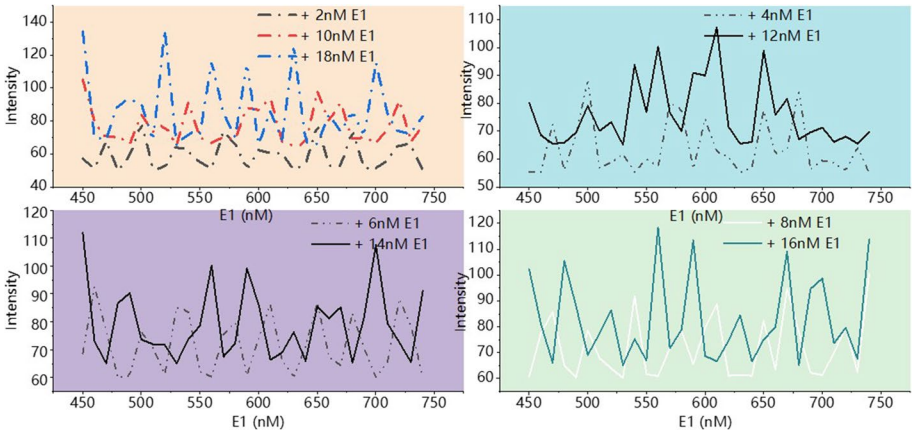

Fig. 3 Fluorescence response of AgNCs-dsDNA

Based on this, we chose 5 min as the optimal incubation time after mixing the two in the following experiments. In AgNCs-dsDNA buffer at a final concentration of 1.0 μM, the fluorescence intensity of AgNCs-dsDNA was enhanced to a maximum when the small peptide concentration was 3.0 μM.

To further explore the binding driving force of the QR small peptide and AgNCs-dsDNA, we then tested the potential of the AgNCs-dsDNA solution as a function of the concentration of the E1 small peptide. The initial potential in the presence of buffer containing 1 μM AgNCs-dsDNA alone was − 22.5 mV. With the addition of QR small peptides to the solution, its potential gradually increased and approached the zero axis, indicating that electrostatic interaction is one of the driving forces for the recognition of QR small peptides with AgNCs-dsDNA.

However, considering that the combination of QR peptide and AgNCs-dsDNA not only caused the fluorescence enhancement of AgNCs-dsDNA, but also caused the red shift of the emission peak, we guessed that there is not only an electrostatic force between the two, but also other possible driving force.

Further detailed analysis of the QR small peptide sequence found that it contains a cysteine, so we guessed that this free thiol group may play a role in the response of the small peptide to AgNCs-dsDNA; that is, silver and the cysteine in the small peptide may play a role. The acid sulfhydryl groups are directly covalently linked together.

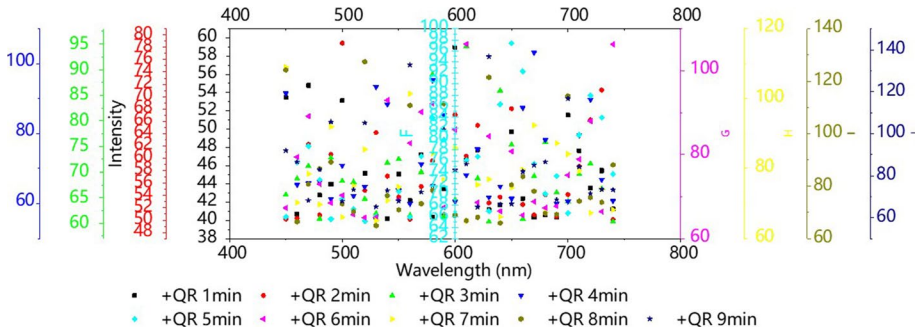

Fig. 4 Detection results of HPV E1 protein with optimized response time

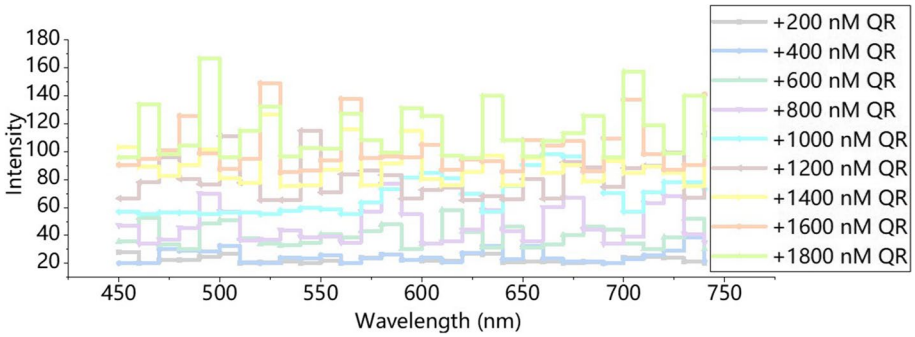

Fig. 5 Detection results of HPV E1 protein with optimized mixed concentration ratio

Next, we performed a control experiment in parallel with N-maleimidoglycine (MAA) as the shielding agent by shielding the sulfhydryl groups in small peptides. Add 20-fold equivalent of MAA to the QR small peptide aqueous solution and incubate for 2 h at room temperature to ensure that the cysteine in the small peptide is completely shielded by direct binding to MAA. The QR small peptides shielded by MAA were added to the buffer containing AgNCs-dsDNA, and their fluorescence spectra were tested after standing for 5 min. As shown in Fig. 6, the fluorescence intensity of AgNCs-dsDNA did not change significantly at this time, proving that the cysteine in the QR small peptide is indeed related to the fluorescence enhancement of AgNCs-dsDNA.

GC and LI are two small peptides with low PI values, and their interaction with AgNCs-dsDNA also leads to the fluorescence enhancement of silver clusters, which indicates that small peptides without positive charges can also interact with AgNCs-dsDNA. Analysis of the sequences of the two shows that the two small peptide sequences both contain 3 cysteines, and for the interaction system of GC and AgNCs-dsDNA, after the cysteine in GC is shielded with MAA, the small peptide does not react. It will cause the fluorescence enhancement of AgNCs-dsDNA. The experimental results of these two small peptides fully demonstrate that the cysteine in the small peptide interacts with AgNCs-dsDNA.

There is no disulfide bond between the 10 cysteines in the E1 protein; that is, the sulfhydryl groups in the protein are all free sulfhydryl groups, so the difference in the number of free sulfhydryl groups is also the E1 protein-AgNCs-dsDNA system. After AgNCs-dsDNA reacted with HPVE1 protein, the fluorescence shift of AgNCs-dsDNA was about 32-nm blue-shift; after AgNCs-dsDNA reacted with low PI, cysteine-rich GC small peptide, the blue-shift of about 29 nm was relatively consistent, which indicated that cysteine played a major role in the response of AgNCs-dsDNA to

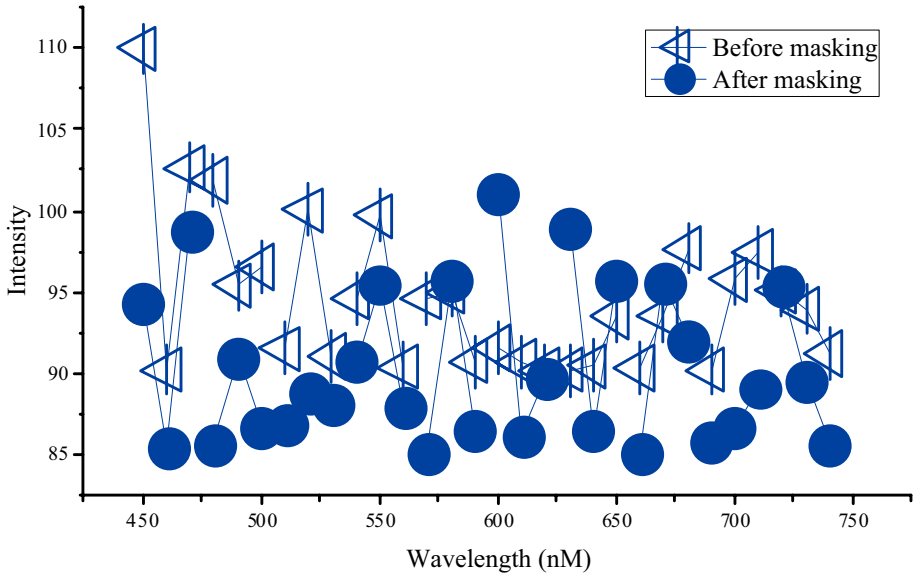

Fig. 6 Fluorescence spectra before and after MAA shielding

HPV E1 protein. The difference between AgNCs-dsDNA and protein and small peptide responses is that the sensitivity of the two is different, the former is a nM-level response, and the latter is a μM-level response. The reasons for this difference may be different cysteines, different surface charges, and the influence of the spatial structure of the protein. That is to say, the response process of AgNCs-dsDNA and E1 protein is the result of the synergistic effect of various factors, but the effect of cysteine and AgNCs-dsDNA is dominant.

GO Enrichment Analysis of Differentially Expressed Gene Functions

According to the results of differential gene detection, we further classified and enriched the obtained data. A total of 5 653 DEGs were screened for GO functional classification annotation and enrichment in T10 vs NC group, of which 4 489 DEGs were annotated in biological process, 474 in cellular component, and 690 in cellular component. Annotated to molecular functions, the functions most enriched for DEGs include immune system processes, stress responses, immune responses, body responses to organics, and cellular responses to chemical stimuli. A total of 3 007 DEGs in the T100 vs NC group were screened for GO functional classification annotation and enrichment, of which 2400 were annotated into biological processes, and 294 into cellular components. The most enriched functions of DEGs include metabolic processes, the body's response to organic matter, the cell's response to organic matter, intracellular information transmission, and programmed cell death. The results of GO enrichment in the T200 vs NC group are shown in Fig. 7.

KEGG Enrichment Analysis of Differential Genes

The biological behavior of organisms is coordinated by a variety of proteins. KEGG pathway enrichment analysis is based on the public database KEGG to further understand the biological functions of differential genes, which is helpful to further verify and clarify the biological regulation mechanism of proteins. According to the KEGG enrichment analysis of differential genes, the five signal pathways with the highest risk factor among the main enriched signal pathways of differential genes in T10 and NC groups include influenza A

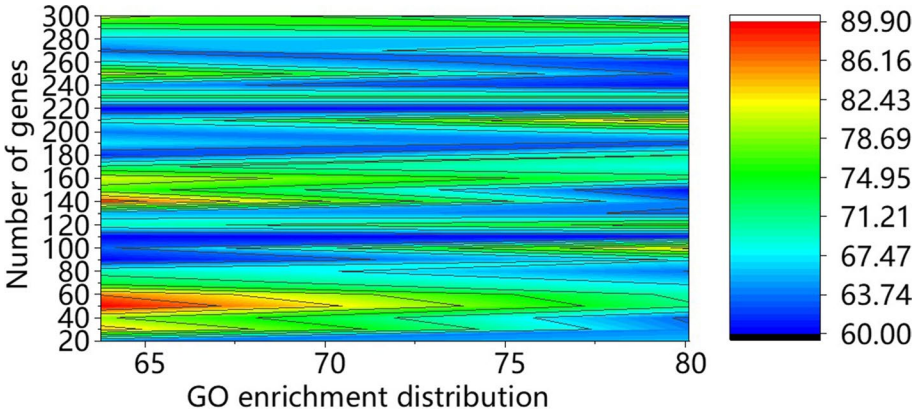

Fig. 7 Results of GO enrichment in T200 vs NC group

virus infection pathway, herpes simplex virus infection pathway, metabolic pathway, and toll-like receptor. The five signaling pathways with the highest risk factor among the main enriched signaling pathways of differential genes in T100 and NC groups include influenza A virus infection pathway, measles infection pathway, JAK-STAT signaling pathway, and endoplasmic reticulum. The 5 signaling pathways with the highest risk factor among the main enriched signaling pathways of differential genes in T200 and NC groups include influenza A virus infection pathway, measles infection pathway, herpes simplex virus infection pathway, and RIG_I receptor signaling pathway. The differential gene KEGG enrichment is shown in Fig. 8.

After transfection with different concentrations of BLV-miR-B4-3p mimics, the mRNA expressions of IL-4, IL-6, and IL-10 in lymphocytes all decreased, but IL-10 transfected BLV-miR-B4. When the amount of 3p mimics reached 200 pmol, the mRNA expression of IL-27 showed a significant upward trend in the three transfection gradients ($P < 0.001$), and the mRNA expression of IL-10 showed a significant downward trend ($P < 0.05$). The mRNA expression of other groups showed a decreasing trend, but there was no significant difference ($P > 0.05$).

The results of 4 genes verified by qPCR of BLV-miR-B4-3p target genes showed that the expression of 3 mRNAs was inhibited, but not all concentrations showed a trend of inhibition, indicating that there are still some errors in the prediction results of target genes.

Discussion

Discussion on the Conformation of Viral Capsid Proteins Induced by HPV Neutralizing Antibody Binding

In the natural state, not all antibodies induced by an antigen can perfectly match the antigen in spatial structure, but the antigen and antibody may have an allosteric effect before and

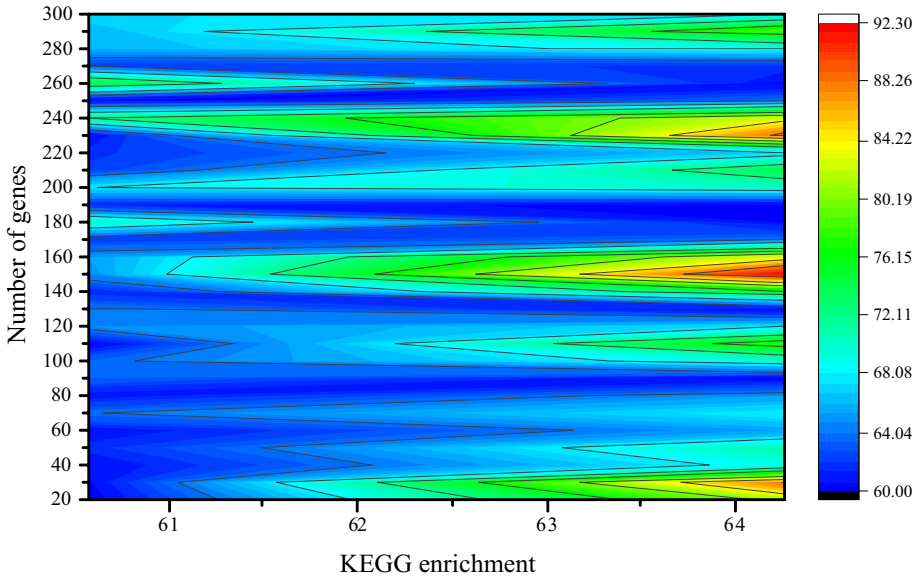

Fig. 8 KEGG enrichment of differential genes

after combining with each other [9]. The binding of antigen or antibody will lead to adaptive changes in the conformation of the binding region on the antigen or antibody, thereby increasing the affinity of the antigen and antibody [10]. In this study, because we analyzed the structures of high-resolution immune complexes HPV58p:A12A3 and HPV59p:28F10 respectively, and also analyzed the crystal structure of HPV58 pentamer, in addition, we also analyzed the HPV59 pentamer in the previous study. The bulk crystal structure was obtained, so we were able to observe the conformational changes induced by the antigen produced by the two antibodies during the binding process.

It was found by fluorescence spectroscopy that after adding HPV E1 protein to the buffer of AgNCs-dsDNA, the fluorescence of AgNCs-dsDNA was enhanced and blue-shifted.

Among them, the structural comparison of the HPV58 capsid protein before and after binding the antibody A12A3 showed that after the HPV58 pentamer was bound to the antibody A12A3, there would be obvious allosteric phenomenon in DEloop, which was exactly consistent with the epitope region recognized by A12A3, because antibody A12A3 mainly binds to DEloop of capsid protein; similarly, after HPV59 capsid protein binds to antibody 28F10, the conformation of FG loop will undergo significant adaptive changes to better bind antibody [11–13]. Another reason for the difference between the antigen conformation after antibody binding and the antigen conformation in the natural state may be that the structure of the antigenic epitope aggregation region on the HPV capsid protein is flexible, and the antigen binding region is fixed in a certain type of antigen after antibody binding [14]. No matter what causes the allosteric effect on the antigen, further study of the occurrence process of this phenomenon, so as to understand the allosteric mode of the HPV virus antigen in inducing the body to produce neutralizing antibodies, will help to target De novo design of functional HPV vaccine IE marker molecules [15].

Spatial Localization and Functional Discussion of HPV Type–Specific Neutralizing Epitopes

Studies on a variety of different virus life cycles have shown that the use of functional antibodies of viruses, especially related antibodies that block the binding of viruses to receptors or affect the occurrence of an event in the process of virus infection, elucidate their recognition at the molecular level [16]. The neutralization pattern of viral antigens, revealing the functional epitope information of antibodies, is of great significance for understanding the process of viral infection, especially the initial stage of viral infection [17]. In the early studies, since the molecular biotechnology for analyzing the structure of biological macromolecular complexes is not very mature, the research on the neutralizing epitopes of important HPV antibodies is mainly through antigenic site-directed mutation or epitope loop region in different types [18]. It was carried out by biochemical means such as homologous replacement between others. Through the research at that time, it was basically determined that the region where HPV induced the body to produce high neutralizing antibody response was mainly located in the five loop regions on the particle surface [19]. However, HPV neutralizing antibodies are mostly epitope conformational antibodies, and due to the limitations of experimental methods at that time, most of the identified epitope information is incomplete. Several intermediate-resolution cryo-EM structures of antibody complexes reported in recent years have further explained the binding mode of antibodies more clearly from the spatial structure [20]. However, due to the limitation of structural resolution, the identified antibody-binding epitope regions are less. The epitope has more than 15 amino acids, generally spanning three to four surface loop regions, which

undoubtedly makes the functional exploration of the epitope in the next step also a huge experimental difficulty [21].

The high-resolution immune complex crystal structures of two representative HPV-neutralizing antibodies were analyzed, and the neutralizing epitopes of the two HPV-neutralizing antibodies were found to be only 6–7 amino acids on the main viral capsid protein [22]. It improves the accuracy of epitope space structure and reduces the difficulty of next functional exploration. Next, we used the precise epitope information of these two antibodies to perform alanine scanning on HPV pseudoviruses to construct multiple mutant pseudoviruses. Sites D154, S168, and N170 and sites M267, Q270, E273, Y276, K278, and R283 on the HPV59 capsid protein play an important role in two types of virus infection. Using this information, we believe that two antibodies were in neutralization mode.

We did not conduct a more in-depth study of the specific functions of these epitope sites affecting viral infection in this paper. Previous studies on HPV infection have shown that the entire process of HPV infection and invasion of host cells requires the participation of multiple cellular receptors and the conformational changes of capsid proteins. Regarding the biological functions of amino acids, we still need to conduct more detailed studies on the binding of mutant pseudoviruses to receptors at the cellular level targeting multiple identified sites that affect viral infection.

Discussion of Cellular Gene Expression Polymorphisms

A total of 34 nucleotide mutation sites were found in the E1-E7 gene variant sequence, among which A176C, A180C, T353C, G391C, T544C, C747T, A759G, and C793T single nucleotide mutation sites have not been reported before [23]. The study found that there are 11 and 28 single nucleotide mutations in HPV52 E1-E7 genes in some regions, indicating that there are differences in the mutation characteristics of HPV52 E1 and E7 genes in different regions [24]. In the process of infection and inheritance, the E1 and E7 gene mutations in this region are relatively active. G350T, A379G, C751T, and A801G are high-frequency mutation sites in HPV52 variant sequences, and the distribution of these high-frequency mutation sites in the population has a certain degree of generality, when E1 and E7 genes selected as targets for diagnosis and treatment have important meaning [25]. The K93R amino acid variant resulting from the A379G mutation is associated with an increased risk of cervical cancer in Korean women, but not in the Chinese population. It can be seen that due to geographical differences, the same amino acid variation may lead to differences in pathogenicity. 52HB01 and 52HB02 are the most dominant variant sequences in this region [26].

Therapeutic vaccines stimulate cellular immune responses and have beneficial therapeutic effects in infected women by arresting disease progression and inducing disease regression [27]. E1 and E7 proteins are consistently overexpressed in cervical tumors and are ideal targets for therapeutic HPV vaccines [28]. Modern bioinformatics techniques can be used for T cell and B cell epitope prediction for peptide vaccine research. At present, epitope prediction mainly focuses on HPV16 and HPV18 subtypes [29]. The detection rate of HPV52 in cervical cancer patients is high, so the epitope prediction and research of HPV52 therapeutic vaccine is urgent. In this study, the T cell epitopes of HPV52 E1 and E7 proteins were predicted, and the dominant epitopes with strong affinity for E1 and E7 proteins in this region were screened [30].

Conclusion

Using the fluorescence enhancement phenomenon caused by the specific recognition and interaction between AgNCs-dsDNA and HPV E1, the effective detection of HPV E1 in vitro was carried out, and the recognition mechanism was further studied. This method is not only convenient to operate and has good selectivity, but also has a detection limit as low as 0.886 nM; in addition, the detection results of AgNCs-dsDNA for E1 show that this method has strong practical application value, which is helpful for the early diagnosis of HPV-related malignant diseases. Studies have shown that IL-27 is a member of the IL-6/IL-12 cytokine family, which can induce a decrease in the expression of Th2-type cytokines, and the decrease in the expression of Th2-type cytokines can inversely lead to an increase in the expression of Th1-type cytokines. It leads to abnormal autoimmune function of the body. The production of cytokines by Th1 and Th2 cells is one of the important ways for the body to regulate autoimmune function. Based on this, we examined the transcriptional expression levels of Th1 and Th2 cytokines by qPCR to explore the effect of BLV-miR-B4-3p on the body's autoimmune function. The expression of Th2 cytokines can inhibit the proliferation of Th1 cells and play a role in humoral immunity. After BLV-miR-B4-3p reaches lymphocytes, the overall expression of Th2 cytokine mRNA tends to decrease, which reduces the humoral immune function of the body. It also increases the risk of developing autoimmune diseases in the body. BLV-miRNAs have the risk of transboundary regulation of human cellular structure and gene expression related to tumor diseases. BLV-miR-B4-3p can activate multiple viral infection pathways in human lymphocytes and lead to abnormal transcription of cytokines, affecting the body's immune function.

Acknowledgements The authors are thankful to the higher authorities for the facilities provided.

Data Availability The data used to support the findings of this study are available from the corresponding author upon request.

Declarations

Ethical Statement Ethical statement not required for this research.

Consent to Participate Not applicable.

Consent to Publish The corresponding author give my consent for the publication of identifiable details within the article to be published in the Journal.

Conflict of Interests The authors declare no competing interests.

References

1. Doorbar, J. (2018). Host control of human papillomavirus infection and disease. *Best Practice & Research Clinical Obstetrics & Gynaecology, 47*, 27–41.
2. Graham, S. V. (2016). Human papillomavirus E2 protein: Linking replication, transcription, and RNA processing. *Journal of Virology, 90*(19), 8384–8388.
3. Gutierrez-Xicotencatl, L., Salazar-Piña, D. A., Pedroza-Saavedra, A., Chihu-Amparan, L., Rodriguez-Ocampo, A. N., Maldonado-Gama, M., & Esquivel-Guadarrama, F. R. (2016). Humoral immune response against human papillomavirus as source of biomarkers for the prediction and detection of cervical cancer. *Viral Immunology, 29*(2), 83–94.

4. Graham, S. V. (2017). The human papillomavirus replication cycle, and its links to cancer progression: A comprehensive review. *Clinical Science, 131*(17), 2201–2221.
5. Cruz-Gregorio, A., Manzo-Merino, J., & Lizano, M. (2018). Cellular redox, cancer and human papillomavirus. *Virus Research, 246*, 35–45.
6. Passmore, J. A. S., & Williamson, A. L. (2016). Host immune responses associated with clearance or persistence of human papillomavirus infections. *Current Obstetrics and Gynecology Reports, 5*(3), 177–188.
7. Harden, M. E., & Munger, K. (2017). Human papillomavirus molecular biology. *Mutat. Res. - Rev. Mutat. Res., 772*, 3–12.
8. Porter, S. S., Stepp, W. H., Stamos, J. D., & McBride, A. A. (2017). Host cell restriction factors that limit transcription and replication of human papillomavirus. *Virus Research, 231*, 10–20.
9. Anacker, D. C., & Moody, C. A. (2017). Modulation of the DNA damage response during the life cycle of human papillomaviruses. *Virus Research, 231*, 41–49.
10. Lu, X., Jiang, L., Zhang, L., Zhu, Y., Hu, W., Wang, J., & Yan, F. (2019). Immune signature-based subtypes of cervical squamous cell carcinoma tightly associated with human papillomavirus type 16 expression, molecular features, and clinical outcome. *Neoplasia, 21*(6), 591–601.
11. Doorbar, J., Zheng, K., Aiyenuro, A., Yin, W., Walker, C. M., Chen, Y., & Griffin, H. M. (2021). Principles of epithelial homeostasis control during persistent human papillomavirus infection and its deregulation at the cervical transformation zone. *Current Opinion in Virology, 51*, 96–105.
12. Durzynska, J., Lesniewicz, K., & Poreba, E. (2017). Human papillomaviruses in epigenetic regulations. *Mutation Research - Reviews Mutation Research, 772*, 36–50.
13. Doorbar, J. (2016). Model systems of human papillomavirus- associated disease. *The Journal of Pathology, 238*(2), 166–179.
14. Songock, W. K., Kim, S. M., & Bodily, J. M. (2017). The human papillomavirus E7 oncoprotein as a regulator of transcription. *Virus Research, 231*, 56–75.
15. Fuentes-González, A. M., Muñoz-Bello, J. O., Manzo-Merino, J., Contreras-Paredes, A., Pedroza-Torres, A., Fernández-Retana, J., & Lizano, M. (2019). Intratype variants of the E2 protein from human papillomavirus type 18 induce different gene expression profiles associated with apoptosis and cell proliferation. *Archives of Virology, 164*(7), 1815–1827.
16. Songock, W. K., Scott, M. L., & Bodily, J. M. (2017). Regulation of the human papillomavirus type 16 late promoter by transcriptional elongation. *Virology, 507*, 179–191.
17. Klymenko, T., Hernandez-Lopez, H., MacDonald, A. I., Bodily, J. M., & Graham, S. V. (2016). Human papillomavirus E2 regulates SRSF3 (SRp20) to promote capsid protein expression in infected differentiated keratinocytes. *Journal of Virology, 90*(10), 5047–5058.
18. Amador-Molina, A., Trejo-Moreno, C., Romero-Rodríguez, D., Sada-Ovalle, I., PérezCárdenas, E., Lamoyi, E., & Lizano, M. (2019). Vaccination with human papillomavirus-18 E1 protein plus α-galactosyl-ceramide induces CD8+ cytotoxic response and impairs the growth of E1-expressing tumors. *Vaccine, 37*(9), 1219–1228.
19. Bahramabadi, R., Dabiri, S., Iranpour, M., & Kazemi Arababadi, M. (2019). TLR4: An important molecule participating in either anti-human papillomavirus immune responses or development of its related cancers. *Viral Immunology, 32*(10), 417–423.
20. Taghizadeh, E., Jahangiri, S., Rostami, D., Taheri, F., Renani, P. G., Taghizadeh, H., & Gheibi Hayat, S. M. (2019). Roles of E6 and E7 human papillomavirus proteins in molecular pathogenesis of cervical cancer. *Current Protein and Peptide Science, 20*(9), 926–934.
21. Taberna, M., Mena, M., Pavón, M. A., Alemany, L., Gillison, M. L., & Mesía, R. (2017). Human papillomavirus-related oropharyngeal cancer. *Annals of Oncology, 28*(10), 2386–2398.
22. Leal, S. M., Jr., & Gulley, M. L. (2017). Current and emerging molecular tests for human papillomavirus–related neoplasia in the genomic era. *The Journal of Molecular Diagnostics, 19*(3), 366–377.
23. Steinbach, A., & Riemer, A. B. (2018). Immune evasion mechanisms of human papillomavirus: An update. *International Journal of Cancer, 142*(2), 224–229.
24. Vonsky, M., Shabaeva, M., Runov, A., Lebedeva, N., Chowdhury, S., Palefsky, J. M., & Isaguliants, M. (2019). Carcinogenesis associated with human papillomavirus infection Mechanisms and Potential for Immunotherapy. *Biochemistry (Moscow), 84*(7), 782–799.
25. da Costa, R. M. G., Bastos, M. M., Medeiros, R., & Oliveira, P. A. (2016). The NFκB signaling pathway in papillomavirus-induced lesions: Friend or foe? *Anticancer Research, 36*(5), 2073–2083.
26. Chiantore, M. V., Mangino, G., Iuliano, M., Capriotti, L., Di Bonito, P., Fiorucci, G., & Romeo, G. (2020). Human Papillomavirus and carcinogenesis: Novel mechanisms of cell communication involving extracellular vesicles. *Cytokine & Growth Factor Reviews, 51*, 92–98.

27. Langsfeld, E., & Laimins, L. A. (2016). Human papillomaviruses: Research priorities for the next decade. *Trends in cancer., 2*(5), 234–240.
28. Wang, R., Pan, W., Jin, L., Huang, W., Li, Y., Wu, D., et al. (2020). Human papillomavirus vaccine against cervical cancer: Opportunity and challenge. *Cancer Letters, 471*, 88–102.
29. Mallen-St Clair, J., Alani, M., Wang, M. B., & Srivatsan, E. S. (2016). Human papillomavirus in oropharyngeal cancer: The changing face of a disease. *Biochimica et Biophysica Acta - Reviews on Cancer, 1866*(2), 141–150.
30. Weng, S. L., Huang, K. Y., Weng, J. T. Y., Hung, F. Y., Chang, T. H., & Lee, T. Y. (2018). Genome-wide discovery of viral microRNAs based on phylogenetic analysis and structural evolution of various human papillomavirus subtypes. *Briefings in Bioinformatics, 19*(6), 1102–1114.

Publisher's Note Springer Nature remains neutral with regard to jurisdictional claims in published maps and institutional affiliations.

Springer Nature or its licensor (e.g. a society or other partner) holds exclusive rights to this article under a publishing agreement with the author(s) or other rightsholder(s); author self-archiving of the accepted manuscript version of this article is solely governed by the terms of such publishing agreement and applicable law.

Authors and Affiliations

Zifeng Wang[1] · Shimin Guan[1] · Baoguo Cai[1] · Shaofeng Rong[1] · Qianqian Li[1]

✉ Qianqian Li
qqli@sit.edu.cn

[1] Department of Bioengineering, Shanghai Institute of Technology, Shanghai 201418, China